

Electronic Supplementary Information

Contents

1 Device fabrication and droplet generation	1
1.1 Device fabrication	2
1.2 Droplet generation	2
1.3 Chamber	2
2 Biochemical oscillator	2
3 Microscope and bulk fluorescence measurement	2
3.1 Microscopy	3
3.2 Bulk	3
4 Delayed population experiment (Figure 3b of manuscript)	3
5 Plotting of fluorescence trace (Figure 2 of manuscript)	3
6 Tracking and size distribution of droplets	3
7 Measurement and plotting of time-to-peak (Figure 3 of manuscript)	4
7.1 Gaussian fit	4
8 Bulk triplicate	4
9 Temperature sensitivity in bulk	5
10 Thermal gradient of the hot plate	5
11 Model of spatial waves	6
11.1 Kinematic waves	6
11.2 Diffusion waves	7

1 Device fabrication and droplet generation

We used two different devices for the preparation and observation of droplets. While polydimethylsiloxane (PDMS) is a convenient material for the generation of droplets and their short-term observation, we found that it interfered with our biochemical oscillator and could not efficiently prevent evaporation, which was a critical step for consistent long-term experiments.

1.1 Device fabrication

The PDMS microfluidic devices were fabricated using a standard soft lithography method. An ultrathick negative photoresist (SU-8; MicroChem, USA) was spin-coated on a silicon wafer to make a negative master with a height of 75 μm . PDMS was spread on the negative master and cured at 75 $^{\circ}\text{C}$ for 90 minutes. The device was then peeled off and bonded with another layer of PDMS by oxygen plasma. The whole device was baked at 200 $^{\circ}\text{C}$ for 5 hours to render the surface of channels hydrophobic.

1.2 Droplet generation

The device contains one oil inlet and one aqueous inlet. Channels are 75 μm wide. Droplets are generated at a flow focusing junction whose constriction is 25 μm wide. For the oil phase, we used fluorinert (FC-40; 3M) containing 2% (w/w) of a PEG-PFPE surfactant (Raindance, [1]). Flow rates for the aqueous and oil phases were typically between 1 and 15 $\mu\text{l}/\text{min}$. Once formed, the droplets are stabilized by travelling in a long channel (70 mm long, 75 μm wide). Droplets are collected in a pipette tip at the outlet. To obtain compact droplets in fluorinert, we generated droplets during 30 minutes to collect enough of them in the tip. We then pipetted the emulsion from the top of the tip, which consists mainly of droplets because they are lighter than fluorinert.

1.3 Chamber

The collected volume of droplets (10 μl) is poured on a hydrophobic coated (durasurf; HARVES) cover glass (Matsunami). The droplets are gently covered with a 5 mm x 5 mm cut cover glass. To prevent air bubbles from getting inside the chamber and making the glass surface hydrophobic, we poured 1 μl of fluorinert on each glass slide beforehand. Edges of the cut glass are sealed with glue (araldite; Nichiban). The chamber is left at room temperature for 30 minutes to dry the glue. After drying, the surface of araldite is painted to black to suppress fluorescence noise.

2 Biochemical oscillator

We used a synthetic biochemical oscillator reported by Fujii and Rondelez, described in details in [2]. Briefly, the oscillator is encoded on a single strand of DNA (the template) and actuated by three enzymes. Compared to the reported system, we removed Evagreen to avoid its partitioning in the oil phase. We used 216 nM of template labeled by DY530 at its 3' end. The sequence is 5'-C*G*G*CCGAATG-CGGCCGAATG-3', where * represent phosphorothioates backbone modifications. We initiated the reaction with 65 nM of trigger strand (prey, 5'-CATTCGGCCG-3') and 2 nM of predator palindromic strand (5'-CATTCGG-CCGAATG-3').

We used a buffer containing 20 mM Tris-HCl, 10 mM $(\text{NH}_4)_2\text{SO}_4$, 10 mM KCl, 50 mM NaCl, 8 mM MgSO_4 , 0.1 % Synperonic F108 (Sigma aldrich), 200 μM dNTP (New England Biolabs, NEB), 2 μM Netropsin (Sigma aldrich), 4 mM DTT, 500 $\mu\text{g}/\text{ml}$ BSA (Invitrogen) and 6 $\mu\text{g}/\text{ml}$ of ETSSB (NEB).

We used enzymes as following: 600 units/ml of Nb.BsmI (NEB), 30 nM of thermophilic ttRecJf [3], 15 units/ml of Bst polymerase large fragment (NEB).

3 Microscope and bulk fluorescence measurement

In order to follow the evolution of the oscillator, we tagged the DNA template with a fluorophore. When the prey binds to the template to replicate, this modifies the interaction of the fluorophore with its bound DNA strand and leads to a partial quenching of fluorescence of the DY530 dye.

3.1 Microscopy

We used an inverted a microscope (IX71; Olympus) on a shock-absorbing desk (ND-1085SUS; Showa) and detected fluorescence with a CCD camera (DU897E-CSO-BV; Andor Technology). The chamber is incubated on a heated stage (MAT-1002ROG-KX; Tokai Hit) at 45.5 °C. A drop of mineral oil (Sigma) was inserted between the chamber and the stage for good heat conduction. The chamber is fixed horizontally below the heated stage with neodymium magnets in order to position the droplets (which are lighter than the oil phase), as close as possible to the heated stage. Oscillations of fluorescence in droplets are observed with a 4x objective lens every minute with 100 ms exposure time. We use excitation light from a light source (Cool LED pE excitation system; Andover) with adequate filters for the fluorophore.

3.2 Bulk

As a control, we recorded the evolution of fluorescence in bulk volume of the same aqueous reactive mix, with a real-time PCR machine (BioRad CFX). Points are recorded every 2 minutes. The volume of mix is 20 μL , which is several orders of magnitudes larger than the volume of droplets.

4 Delayed population experiment (Figure 3b of manuscript)

After generation, we separated the droplets into 2 groups. One group is kept at room temperature and the other group is incubated at 45.5 °C for 1 hour within a PCR machine (BioRad CFX). After 1 hour incubation, we mixed gently the two groups of droplets with a pipet and transferred this mix to the chamber.

5 Plotting of fluorescence trace (Figure 2 of manuscript)

The traces plotted in Figure 2 of manuscript are processed to facilitate comparison. Each microscopy or bulk trace is normalized to have a mean intensity of 1, detrended to remove linear drift and smoothed with a moving average filter with a window size of 10 minutes. We discarded traces whose maximum was higher than 1.1 or minimum lower than 0.7 (about 30 traces out of 717), which often corresponded to “pathological” traces or possible errors during the tracking process.

6 Tracking and size distribution of droplets

For quantitative analysis of the oscillations, the (possibly moving) droplets were localized and time-tracked using the Crocker&Grier algorithm [4]. We took special care in the background removal step, dividing by a background constant in time rather than by a time-dependent one in order to keep consistent intensities measures. The intensity of each droplet was measured on the blurred and background-removed version of the image as the mean intensity of a 5x5 pixels neighbourhood centered on the localisation of the particle. In order to avoid losing or mis-linking trajectories during the rapid coordinated movement of a block of droplets, we obtained independent information on the advected motion and its spatial dependence via correlation analysis of the raw images and used this information in the trajectory linking process [5].

The size distribution of droplets is shown in Figure 1. We obtained the relative sizes of droplets via the method explained in [6]. We calibrated the absolute size by measuring the average size of a dozen of droplets (90 μm). Gaussian fitting of the distribution yields a dispersion of about 15%. It must be noted that the algorithm gives an upper bound of the polydispersity, as measurement errors widen the real distribution.

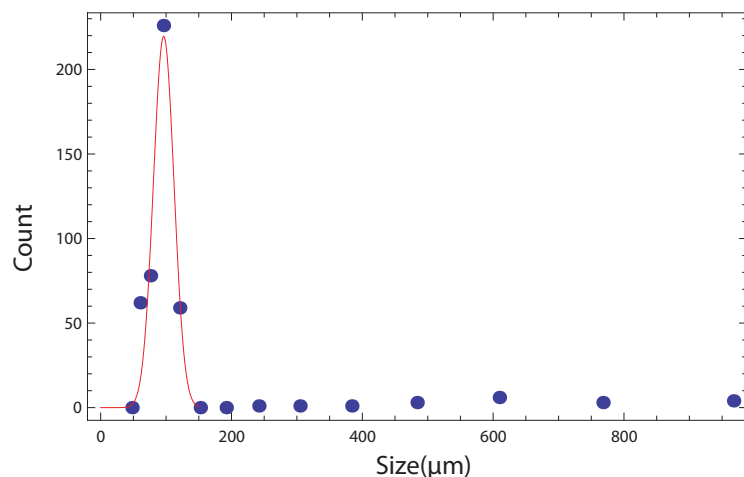


Figure 1: Size distribution of droplets. The fit shows a Gaussian distribution

7 Measurement and plotting of time-to-peak (Figure 3 of manuscript)

In order to find the T_i , we used the raw rather than smoothed traces of Figure 2 of manuscript because the smoothing algorithm broadens and moves the peaks. The timing was found in an iterative way: the position of the $(i + 1)^{th}$ peak T_{i+1} is guessed from T_i and then looked for as the position of the intensity minimum in an interval around the predicted position. The T_i , measured for the 690 traces of Figure 2b of manuscript, are then plotted in a histogram with a bin size of 5 minutes. For the delayed population experiment, sudden moves of droplets were more frequent, which complicated tracking. The tracking algorithm yielded 109 traces, of which 59 proved viable after manual inspection.

7.1 Gaussian fit

As a guide to the eye, we then independently fitted a single Gaussian (Fig.3a of the manuscript) or a sum of two Gaussian distributions (Fig.3b of the manuscript) $h_i(t)$ for each T_i

$$h_i(t) = A_i e^{-\frac{(t-\mu_i)^2}{\sigma_i^2}} \quad \text{or} \quad h_i(t) = A_{1i} e^{-\frac{(t-\mu_{1i})^2}{\sigma_{1i}^2}} + A_{2i} e^{-\frac{(t-\mu_{2i})^2}{\sigma_{2i}^2}}$$

with the condition that the total count be equal to the number of traces represented by the histogram.

$$\sum h_i(t_j) = 690 \quad \text{or} \quad \sum h_i(t_j) = 59$$

where the sum is done over the binned times. We found the free parameters by independently minimizing the quadratic error between h_i and T_i for each i .

8 Bulk triplicate

We also tested the desynchronization of oscillators in bulk. To do this we ran a triplicate of the same reactive mix. As is clear from Figure 2b, the 3 tubes diverge slightly in frequency, with a standard deviation increasing from 2

minutes for T_1 to 6 minutes for T_7 .

9 Temperature sensitivity in bulk

In order to test the effect of temperature on oscillators in bulk, we incubated them at different temperatures (Figure 2a). We find that increasing the temperature by 2°C lengthens the period by 25%.

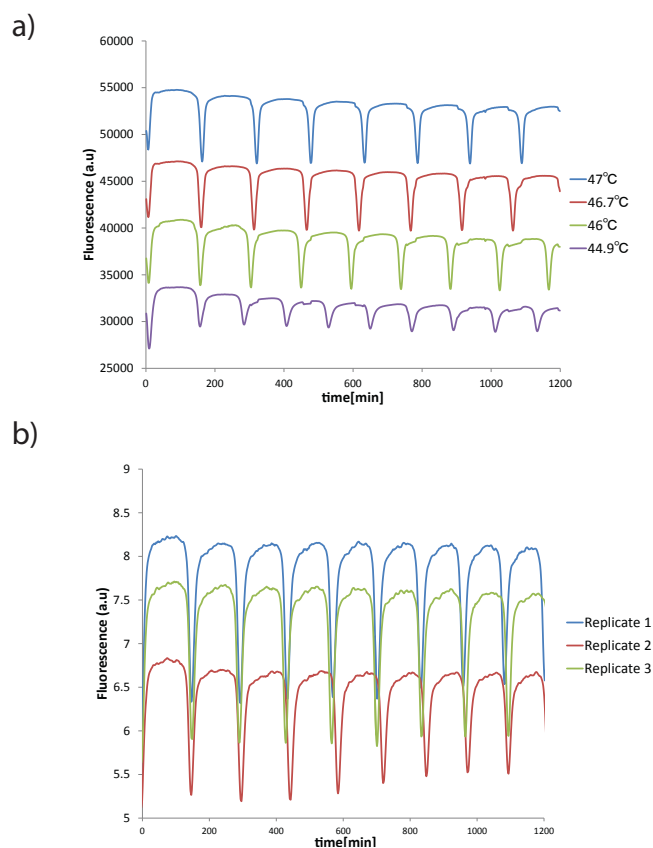


Figure 2: a) Effect of temperature on the period of oscillators in bulk. The oscillators are prepared as described before and incubated at the indicated temperature in a real-time PCR machine. b) Triplicate run of the oscillator, at 45.5 °C

10 Thermal gradient of the hot plate

Figure 3 shows the thermal gradient in the middle of the hot plate. We used a thermal camera (FSV-GX7700 Apiste, Japan) set for the emissivity of a standard glass slide (0.95). The temperature of the plate was set to 45.5 °C and allowed to equilibrate for 5 minutes. Linear regression yields a thermal gradient of 0.15 °K/mm.

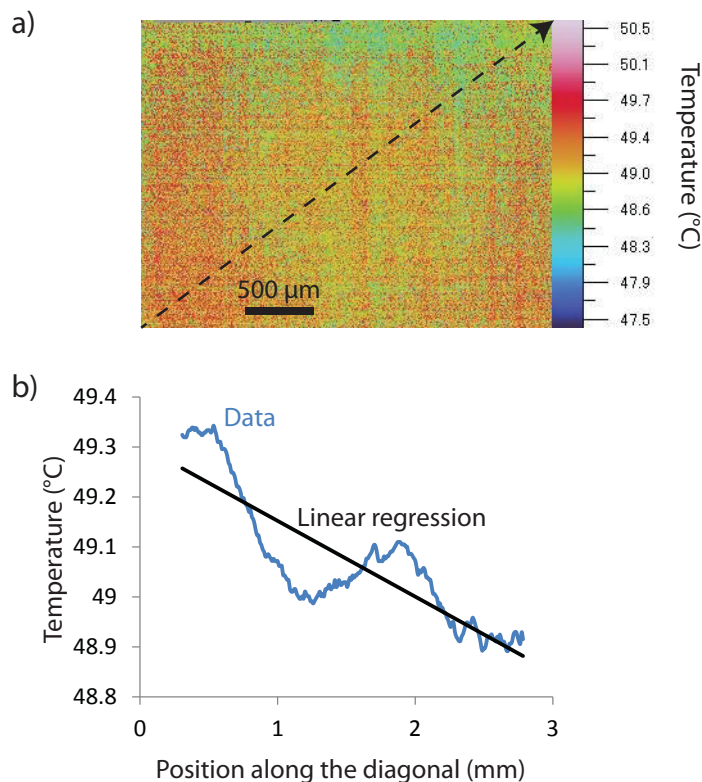


Figure 3: a) Temperature of the hot plate. The plate was set to 45.5 °C. b) Plot of temperature along the diagonal in a), smoothed with a moving average filter with a window of 0.6 mm. The straight line is the linear regression.

11 Model of spatial waves

In this section, we use the measured speeds of the waves in movie M1 to discriminate the physical effects causing them.

11.1 Kinematic waves

We assume that waves are caused by a spatial gradient of temperature. Droplets at different locations have different temperatures, and will oscillate with different periods. This results in the appearance of pseudo-waves because droplets close spatially reach their maximum of fluorescence close in time. Let us denote $T(z)$ the temperature and $P(T(z))$ the period of an oscillator located at position z . Following Kopell and Howard [7], an ensemble of oscillators initially synchronized will display a sequence of decelerating waves, where the speed of the n^{th} wave is

$$v_n = \frac{1}{n |\nabla P(T(z))|} = \frac{1}{n \left| \frac{dP}{dT} \right| \left| \frac{dT}{dz} \right|}$$

where $\left|\frac{dP}{dT}\right| = 15.6 \text{ min}/K$ is the sensitivity of the period to temperature (measured in bulk in section 9) and $\left|\frac{dT}{dz}\right|$ the intensity of the spatial gradient.

11.2 Diffusion waves

In the diffusion model, waves result from transport of reagents. Convection is neglected as the milieu is not stirred (although droplets occasionally move). We model the ensemble of droplets as a continuous medium in which DNA strands diffuse with an apparent diffusion coefficient D_p , which aggregates diffusion inside and between the droplets. The concentration of other reagents (enzymes, buffer) is assumed to be homogenous spatially.

Padirac et al. have studied the emergence of waves due to diffusion in such unstirred and continuous medium [8]. They predict a minimal speed for a wave of

$$v_{min} = 2C\sqrt{D_p k_2 pol K_{m,p}} \quad (1)$$

where $C = 1.3$, $pol = 1.85 \text{ nM}$ is the concentration of polymerase, $k_2 = 4 \times 10^{-3} \text{ nM}^{-2} \text{ min}^{-1}$, and $K_{m,p} = 34 \text{ nM}$ is the Michaelis-Menten constant for the polymerase. Equating the speed of (1) with the minimum observed wave speed ($55 \text{ }\mu\text{m}/\text{min}$, wave number 4), we obtain an estimate on the apparent diffusion coefficient

$$D_p = 1800 \text{ }\mu\text{m}^2/\text{min}$$

For such diffusion coefficient, it would take about 5 minutes for a strand of DNA to diffuse to an adjacent droplet, for droplets of size $100\text{ }\mu\text{m}$.

References

- [1] C. Holtze, A. C. Rowat, J. J. Agresti, J. B. Hutchison, F. E. Angile, C. H. J. Schmitz, S. Koster, H. Duan, K. J. Humphry, R. A. Scanga, J. S. Johnson, D. Pisignano, and D. A. Weitz. Biocompatible surfactants for water-in-fluorocarbon emulsions. *Lab on a Chip*, 8(10):1632–1639, 2008.
- [2] Teruo Fujii and Yannick Rondelez. Predator-prey molecular ecosystems. *ACS Nano*, 7(1):27–34, 2013.
- [3] A. Yamagata, R. Masui, Y. Kakuta, S. Kuramitsu, and K. Fukuyama. Overexpression, purification and characterization of recj protein from thermus thermophilus hb8 and its core domain. *Nucleic Acids Research*, 29(22):4617–4624, 2001.
- [4] J. C. Crocker and D. G. Grier. Methods of digital video microscopy for colloidal studies. *Journal of Colloid and Interface Science*, 179(1):298–310, 1996.
- [5] R. Besseling, L. Isa, E. R. Weeks, and W. C. K. Poon. Quantitative imaging of colloidal flows. *Advances in Colloid and Interface Science*, 146(1-2):1–17, 2009.
- [6] M. Leocmach and H. Tanaka. A novel particle tracking method with individual particle size measurement and its application to ordering in glassy hard sphere colloids. *Soft Matter*, 9(5):1447–1457, 2013.
- [7] N. Kopell and L. N. Howard. Horizontal bands in belousov reaction. *Science*, 180(4091):1171–1173, 1973.
- [8] Adrien Padirac, Teruo Fujii, Andre Estevez-Torres, and Yannick Rondelez. Spatial waves in synthetic biochemical networks. *Journal of the American Chemical Society*, Article ASAP:DOI: 10.1021/ja403584p, 2013.